Beam Squint Exploitation for Linear Phased Arrays in a mmWave Multi-Carrier System

Ignas Laurinavičius, Huiling Zhu, Jiangzhou Wang and Yijin Pan
Department of Engineering and Digital Arts, University of Kent
Email:{il79, H.Zhu, J.Z.Wang, Y.Pan}@kent.ac.uk

***Abstract*—To support millimeter-wave (mmWave) communications successfully, a large number of antennas (in the order of hundreds or thousands) must be implemented to mitigate significant propagation and scattering losses. Designing phased arrays for carrier frequency is a great method for narrowband systems, but the performance degrades significantly with larger bandwidth. We show that as the system bandwidth increases, the beams steer away from the focus direction, which is an effect known as beam squint in wideband systems. In this paper, at first, analysis of capacity is performed for an increasing number of antennas, to show the significance of beam squint. Then, a solution in digital domain is proposed. Conventionally, a single beam would be allocated to a user. By exploiting beam squint effect, in this solution more than one beam can carry a single-user's data, which improves the system's performance significantly, especially when the number of antennas in an array is large and there are multiple users.**

I. Introduction

At 30-300GHz, the communication spectrum is much wider than for current technologies [1]. Therefore, increasing frequency spectrum availability to millimeter wave (mmWave) become one of the research frontiers for the next generation of communications, which allows mobile operators to access the spectrum with wide bandwidth to achieve high data rate. Note that at such frequencies, signals suffer from a much higher path-loss than systems operating at less than 6GHz. mmWave also experiences small-scale fading due to particle presence in the channel and even oxygen or rain can attenuate the signals tremendously [2]. Due to these factors, using antenna array to form narrow beams is adapted as a solution for mmWave systems to achieve a coverage similar to sub 6GHz bands.

Phased array is one of the popular choices due to its low complexity. However, phased arrays are only a good implementation for narrowband systems, as phase shifters can be configured at only the carrier frequency. That is, the configuration of an approximation assuming phase shifter values remains stationary for all transmission frequencies, as there are practical limitations, such as the cost of hardware. Then only approximated performance could be obtained at frequencies other than the carrier frequency, which does not work well for wideband implementation. If the Angle of Arrival(AoA) or Angle of Departure(AoD) of a signal is not on the broadside, i.e. not 0 degrees, the beam direction is frequency dependent. Any beam that is transmitting or receiving over a frequency that is not the carrier frequency gets steered away (squinted) as a function of frequency. In a wide bandwidth this results in much smaller gains at edge frequencies. This phenomenon is known as beam squint. In a multi-carrier system, e.g. orthogonal frequency division multiplexing (OFDM) [3],[4], for a given user position, beam squint can be portrayed more easily as an array of different gains as a function of frequency or subcarrier index number.

Currently there are only a few methods in solving the beam squint issue. True Time Delays (TTD) [5] is a hardware solution, suggesting an implementation of TTD circuit elements that would make phase shifting frequency independent even over wider frequency bands. However, this solution is undesirable in massive multiple input multiple output (mMIMO), co-located or distributed[6], as when the number of phase shifters and antennas is very large, the power consumption, implementation cost and circuit complexity scale make it impractical. Another method [7] was proposed to increase the density of a codebook to combat the beam squint effects, which is more practical. However, having very large codebooks can lead to long beamforming times, introducing latency. Other studies were performed on hybrid beamforming systems [8],[9] and as such introduced extra flexibility into the system through a digital precoder. The latency and complexity of the system could be very high due to the adaptation of a digital precoder, especially in a system with multiple users. Therefore, it is important to study the beam squint problem and look for more efficient ways of solving it to reduce the latency introduced by the codebook based solution and implementation complexity that is associated with the hardware solution. Therefore, this paper aims to minimize the implementation cost of beam squint mitigation by studying analog beamforming, and a subcarrier to beam allocation scheme is proposed to improve the throughput.

This paper's contributions are two-fold. Firstly, an analysis is performed to show how the change in number of antennas affects beam squint and how wideband beam squint alters the conventional narrowband models. Secondly, based on the performance analysis, a subcarrier to beam allocation scheme is proposed by integrating two novel cooperative algorithms. One algorithm estimates the amount of beam squint in the system and locates best beams for allocation in a multi-carrier implementation, while the second algorithm maps data to the respective beams. Simulation results show a significant increase in performance when it comes to the reliability of the system as well as the capacity. The solution at the very least eliminates the antenna and bandwidth limiting effects of beam squint.

The remainder of this paper is structured as follows. Section

978-1-7281-0962-6/19/$31.00 ©2019 IEEE

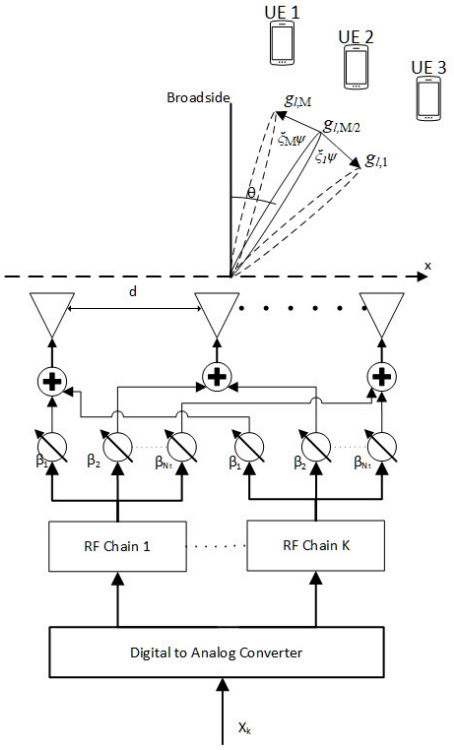

Fig. 1. ULA used for analog beamforming. Beam squint effect demonstrated in a multi-user scenario.

II presents the system model, introducing the transmission system used as well as the beam squint. Section III analyses the problem and presents a novel scheme that exploits beam squint to improve performance. Section IV presents simulated performance of the proposed scheme. Conclusions are drawn in Section V.

II. System Model

A. Analog Beamformer

Consider an OFDM mMIMO system with N_t transmit antennas and M subcarriers indexed $m = 1, 2, \cdots, M$. The N_t antennas are deployed in the shape of a Uniform Linear Array(ULA), as shown in Fig. 1. Number of radio frequency (RF) chains determines how many users' data streams can be scheduled at a single time instance. All antennas are isotropic, and of the same shape. Denote λ_c as the wavelength of the carrier frequency, f_c. The distance d between two adjacent antenna elements is set to be half wavelength, i.e. $d = \lambda_c/2$. AoD or AoA is denoted as θ, relative to the broadside. The angle increases clockwise, and the analytical limit is $\theta \in [-\frac{\pi}{2}, \frac{\pi}{2}]$. We will define a virtual angle ψ to keep expressions shorter, which is given by

$$\psi = \sin\theta. \tag{1}$$

Denote β_n as a phase shift value of the nth antenna element. The phase shifters are implemented in a beamforming vector, which is denoted as

$$\mathbf{w} = \left[e^{j\beta_1}, e^{j\beta_2}, \cdots, e^{j\beta_{N_t}}\right]^T. \tag{2}$$

With the carrier frequency f_c, given a target angle θ_F, the goal of a beamforming system is to maximise the array gain towards angle θ_F, which can be converted to ψ_F following (1). The goal can be achieved by setting up phase shifters to ensure all of the N_t antenna elements have the same time-delay for receive or transmit signals, at the carrier frequency f_c , which is a solution for optimal implementation cost of the system in a multi-carrier environment. Following [10], to focus on an angle ψ_F, the phase shifter configuration is given by

$$\beta_n(\psi_F) = 2\pi \cdot \lambda_c^{-1} \cdot d \cdot (n-1) \cdot \psi_F,\ n = 1, 2, \cdots, N_t, \tag{3}$$

Corresponding to the beamforming vector $\mathbf{w}$ for any frequency f the ULA response vector at any angle θ is derived as

$$\begin{aligned}\mathbf{a}(\theta) = \Big[1, e^{j2\pi\lambda^{-1}1d\psi}, e^{j2\pi\lambda^{-1}2d\psi}, \cdots, \\ e^{j2\pi\lambda^{-1}(N-1)d\psi}\Big]^T, \psi \in [-1, 1].\end{aligned} \tag{4}$$

Then, based on the array response vector $\mathbf{a}(\theta)$ at frequency f, and pre-designed beamforming vector, $\mathbf{w}$, the array gain normalized by the square root of number of antenna elements N_t is given by

$$g(\mathbf{w}, \theta) = \frac{1}{\sqrt{N_t}}\mathbf{w}^H\mathbf{a}(\theta) = \frac{1}{\sqrt{N_t}}\sum_{n=1}^{N_t} e^{j[2\pi\lambda^{-1}(n-1)d\psi - \beta_n]} \tag{5}$$

where $(\cdot)^H$ denotes the Hermitian transpose.

B. Beam Squint Model

As stated before, phase shifters are designed for the carrier frequency, meaning that they are fixed, regardless of operating frequency, within bandwidth B. This introduces beam squint. Beam squint can be effectively defined as the ratio ξ of operational frequency f to the carrier frequency f_c

$$\xi = \frac{f}{f_c}, \tag{6}$$

where $f \in \left[f_c - \frac{B}{2},\ f_c + \frac{B}{2}\right]$. Then, the fractional bandwidth is defined as

$$b = \frac{B}{f_c}. \tag{7}$$

and $\xi \in \left[1 - \frac{b}{2},\ 1 + \frac{b}{2}\right]$. Since ξ is dependent on b, any reduction in b will reduce the range of ξ available. For example, in a wide bandwidth of 2.5GHz with a center frequency 73GHz (considered as the carrier frequency), ξ varies from 0.9829 to 1.0166. Fig. 2 demonstrates that the gain at edge frequencies is much smaller than at the center frequency, for a large number of antennas $N_t = 256$. Any frequency corresponding to gains that are 3dB or more smaller than maximum gain is considered unusable for transmission to the user. In [10], the array gain derived in (5) is modified for a subcarrier with a ratio ξ, AoA/AoD ψ, and beam focus angle ψ_F. This is expressed as $g(\xi\psi - \psi_F)$, where

$$g(x) = \frac{\sin\left(\frac{N_t\pi x}{2}\right)}{\sqrt{N_t}\sin\left(\frac{\pi x}{2}\right)}e^{j\frac{(N_t-1)\pi x}{2}} \tag{8}$$

A subcarrier with ξ at AoA/AoD ψ has a gain equivalent to a gain for the carrier frequency f_c at AoA/AoD $\psi' = \xi\psi$. The maximum array gain is achieved by

$$g_{max} = \max_{\psi\in[-1,1]} g(\psi - \psi_F) = \sqrt{N_t} \tag{9}$$

It can be seen that at frequency f, the maximum array gain is achieved at angle $\psi = \psi_F/\xi$, which makes the beam steer away from the focus angle ψ_F when $\xi \neq 1$, i.e. $f \neq f_c$. The beam squint effect is illustrated in Fig. 1. As the bandwidth changes, so does the range of ξ. When the bandwidth is narrow, $\xi \approx 1$ or $|\Delta\xi| \approx 0$, from Fig. 2 this means that the beamforming gain $g \approx \sqrt{N_t}$ for the entire bandwidth. As the bandwidth becomes relatively large e.g. crosses $|\Delta\xi| = .008$ the performance is optimal for a small range of frequencies around the centre, but at the edges, when $\xi = 0.9829$ or 1.0166, the gain is approaching the gain of the first sidelobe of the same beam. In Fig. 1 these edge frequencies correspond to the dashed beams.

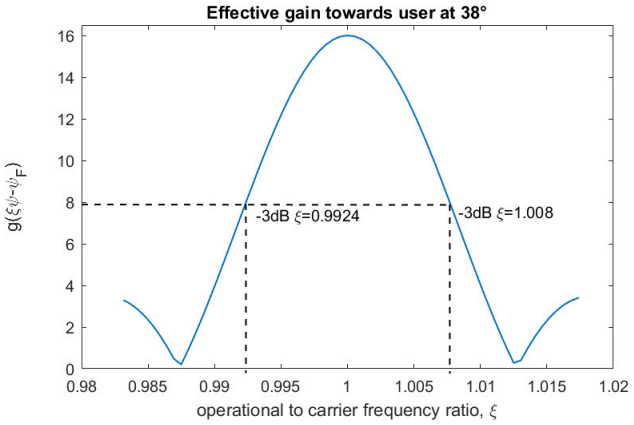

Fig. 2. Effective normalised gain across entire bandwidth in a single-carrier system, $N_t = 256$.

III. Problem Analysis

A. Channel Capacity of OFDM System

In this paper the receiver has only one antenna and only transmitter beam squint is considered. Analysis is performed on multiple user scenarios and a single user implementation with multiple RF chains is studied as a special-case. Equal power is allocated across all subcarriers. This is common under the condition of no channel state information. mmWave bands with narrow beams ensure a sparse channel [2]. As a result, line of sight (LoS) is assured.

Within bandwidth B, before beamforming, the antenna receiving a signal receives power $P = \frac{P_t}{K}$ where P_t is the total power of the system and K is the number of scheduled users. The noise power of AWGN split across M subcarriers is $\sigma^2 = \frac{B}{M}N_0$. The channel capacity for a multiple user OFDM system with Beam Squint at AoD ψ and beam focus angle ψ_F is thus

$$R_{BS} = \sum_{k=1}^{K} \frac{B}{M} \sum_{m=1}^{M} \log\left(1 + \frac{P_t \left|g_k\left(\xi_m\psi_k - \psi_{F,k}\right)\right|^2}{K\frac{B}{M}N_0}\right) \tag{10}$$

where

$$\xi_m = 1 + \frac{(2m - M + 1)\, b}{2M}. \tag{11}$$

and in the beam squint environment, variables $g_k(\cdot)$, and $\psi_{F,k}$ show that the beamforming gain and focus angle, respectively, for a specific user. This specification is important, as, depending on the user location the number of beams available for use, e.g. user k, varies when as beam squint is stronger further away from the broadside. For comparison, the channel capacity for a multi-user system with no beam squint denoted as R_{NBS} is derived. Based on the single user capacity obtained in [10] at AoD θ, and beam focus angle ψ_F, the multi-user system capacity can be simply K times of that achieved in a single user scenario, as without beam squint i.e. $\xi = 1$ for all users, and $g_1 = g_2 = \cdots = g_k = g_{max}$. Therefore the capacity of K users is given by

$$\begin{aligned} R_{NBS} &= \sum_{k=1}^{K} B\log\left(1 + \frac{P_t\left|g_{max}\right|^2}{K\frac{B}{M}N_0}\right) = \\ &= KB\log\left(1 + \frac{P_tN_t}{K\frac{B}{M}N_0}\right). \end{aligned} \tag{12}$$

To solve for a single user environment, set $K = 1$. Both R_{NBS} and R_{BS}, achieve under the scenarios without and with beam squint, are maximised if $\psi_k = \psi_{F,k}$. Fig. 6 shows a comparison of capacity in the two scenarios as the number of antennas increases with given $SNR = 12$dB. It can be seen from Fig. 6 that R_{NBS} shows an expected rise in performance, as more antennas produce higher gain towards a single user when no beam squint is present in the system. Convergence is being approached as there is a power constraint in the system which limits the capacity as the number of antennas increases. As the negative effect is introduced, in both single and multi user scenarios beam squint starts affecting the system negatively from the very beginning. Despite this, a rising trend up until around 100 antennas is observed for a single user scenario, while the multiple user case reaches a maxima at 64 antennas. Once that limit is reached, the system performance staggers and the capacity for beam squint scenarios starts decreasing. A stronger fall in performance on multi-user is shown, as the rises and falls are K times stronger in the multi-user case. Fig. 3 shows a comparison of both scenarios by measuring the maximum achievable throughput as a function of fractional bandwidth defined in (7). As fractional bandwidth increases, the range of values that ξ can undertake extends, which leads to strengthening the beam squint effect. As such, while the gain is constant for the R_{NBS} scenario, the throughput does not change, however as beam squint is introduced for the R_{BS} scenario, the capacity degrades significantly as the bandwidth increases. This shows that beam squint effects for wide communication bandwidths are a significant issue.

IV. Maximum Gain Stream Allocation

A. Subcarrier to Beam Allocation

When serial data containing K users' data enter the transmission system, conventionally these data will be distributed to

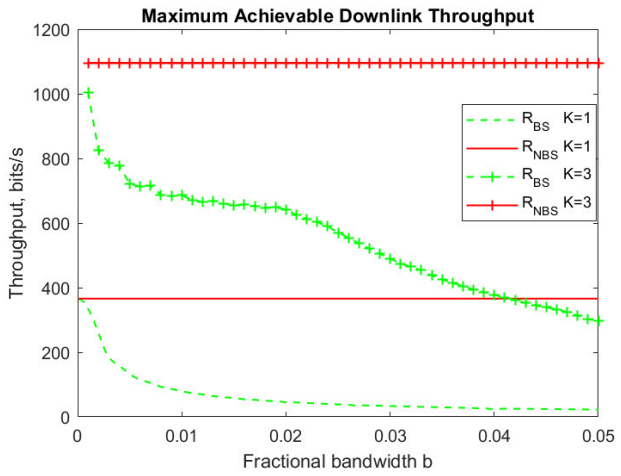

Fig. 3. Achievable downlink throughput as a function of fractional bandwidth in a single and a multiple user scenario. Number of antennas $N_t = 256$.

each respective user and their exclusively assigned beams. Due to beam squint effects, the data transmitted will suffer heavy losses on a high number of subcarriers assigned to each users. Hence in the paper, a subcarrier-to-beam allocation (SBA) scheme is proposed, which acquires information about beam squint and uses this information to maximise the gain $g_k(x)$ towards any given user. The scheme is proposed based on the concept of interleaving. The input data, as the input of each single beam, will be split across $L_k < N_t$ beams, and this may result as some data of a user, e.g. user k, being mixed in with other users' data on the beams allocated to them. A beam may not be exclusively allocated to one user. Given a user, due to beam squint effects, the edge subcarriers would have the beams to point away from the user and result in degraded gains. As the beam pattern is fixed, for the purpose of interleaving, given a user, SBA algorithm selects L significant beams, according to the information of the number of beams present within an angle range given by $\theta_{max}(f) \in [\theta_F - \Theta_s, \theta_F + \Theta_s]$, where

$$\Theta_s = |\theta_{max}(f) - \theta_F| = \left| \sin^{-1}\left(\frac{\sin(\theta_F)}{1 + \frac{f}{fc}} \right) - \theta_F \right| \qquad (13)$$

and $f \in \left[-\frac{B}{2}, \frac{B}{2}\right]$ is the operating frequency relative to carrier frequency. Then, interleaving will be carried out among the L_k selected beams for the data of user k. Therefore, the number of selected beams, L_k, would affect the system performance. In the SBA, a gain difference factor, $e_{l,m}(\theta)$, is defined for each beam at AoD θ to find a suitable subcarriers for transmission across all chosen beams, which is given by

$$e_{l,m}(\theta) = \frac{g_{l,m}(\theta) - g_{max}}{g_{max}} \qquad (14)$$

where $g_{l,m}(\theta)$ is the gain of beam l on subcarrier m at a given angle θ. Each subcarrier that has gain difference factor higher than a pre-defined threshold e_{th} is stored in a subcarrier gain matrix $\mathbf{S} = \{S[l,m] = g_{l,m}(\theta)\}_{L_k \times M}$. After it is generated, $S[l,m]$ is examined, and the beam with the highest gain on subcarrier m, denoted by $l_{k,m}$ is allocated to user k. Its gain is recorded by $G_k[m] = S[l_{k,m}, m]$. The method of allocating subcarriers to beams is summarised in Algorithm 1. Due to the nesting of loops, the complexity of the algorithm for a full user range is $\mathrm{O}(KL_kM)$. None of these variables scale quickly, the number of usable beams for beam squint compensation increases slowly with N_t, number of users that would be available to benefit from the algorithm depends on their spacing and varies between $[1, N_{RF}]$. M can take a multitude of discrete values that can be constant depending on the system and it allows for further simplification of the complexity to $\mathrm{O}(KL_k)$. Fig. 4 illustrates when $K = 3$ and $N_t = 256$ and $M = 64$ for full exploitation of beam squint, the subcarrier gains achieved with $L = 2$ auxiliary beams used. These 2 beams, considering similar beam squint properties, are able to provide the subcarriers unusable due to beam squint from the most significant beam. A comparison of the subcarrier gains achieved by the SBA vs. original subcarrier gains affected by beam squint is shown in Fig. 4. The proposed algorithm increases the average gain two times over the entire subcarrier range. Finally, an allocation set A_k is created, whose elements show a beam allocation for each subcarrier for the kth user, which will enable the interleaving algorithm to map data.

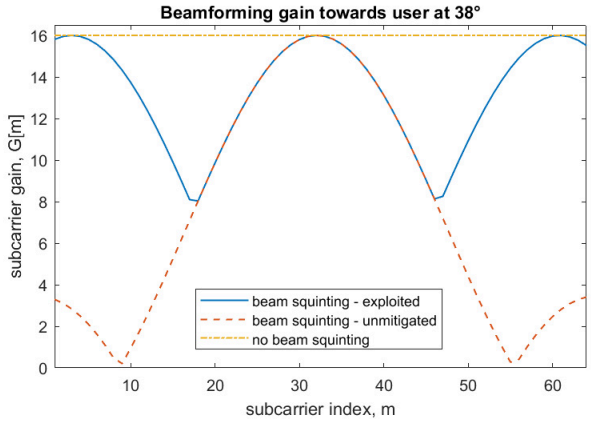

Fig. 4. Subcarrier gain towards a single user for each subcarrier m. N_t=256, f_c = 73GHz, BW = 2.5GHz and $M = 64$. Comparison between the system with no beam squint and with solution (beam squinting - exploited) present for $L = 3$.

B. Data Interleaving

Using information that is returned from Algorithm 1, it is now possible to rearrange input data to ensure it reaches the required beam, to benefit from the possible gains. A second algorithm is proposed to meet this goal. If an ordered arbitrary serial data set $X \in \mathbb{R}$ containing K users' data is to be mapped to beams, conventionally one user's data would only be exclusively allocated to one beam. In the SBA scheme, using Algorithms 1 and 2 will override the selection, as one user may get allocated more than one beam. Then, following Algorithm 1, which has successfully returned a subcarrier to beam allocation set for each user separately, Algorithm 2 is developed for data interleaving, which creates a data allocation indication matrix, or the output stream $\mathbf{D} \in \mathbb{R}^{L \times M \times K}$. The element $d_{l,m,k}$ of $\mathbf{D}$ takes value of one if the beam L is selected

Algorithm 1 Subcarrier to Beam Allocation

Initialise subcarrier index $m = 1$ and user index k
Locate number of beams L_k within Θ_s from main beam.
for all significant beams $l = 1, 2, \cdots, L_k$ **do**
  Calculate phase shifter values β
  Apply $AF[\theta]$ to each phase shifter
  Calculate the gain $g_l[\theta]$
  Normalise gain to number of antenna elements $\frac{g_l[\theta]}{N_t}$
  Find maximum gain $g_{max} = \max g_{l,m}[\theta]$
  for all $g_{l,m}[\theta]$ $m = 1, 2, \cdots, M$ **do**
    if $e_{l,m} = \frac{|g_{l,m}[\theta] - g_{max}|}{g_{max}} \cdot 100 \leq e_{th}$ **then**
      Generate a usable subcarrier gain matrix $\mathbf{S} = \{S[l,m] = g_{l,m}[\theta], l = 1, \cdots, L_k, m = 1, \cdots, M\}$
    end if
  end for
end for
Choose highest gain subcarriers for beam allocation $G_k[m] = \max_l(S[l,m]), m = 1, 2, \cdots, M, l = 1, 2, \cdots, L_k$
Locate beam indexes corresponding to the gains $G_k[m]$, $A_k = \{l_{k,m} = \arg\max_l(S[l,m]), m = 1, 2, \cdots, M, l = 1, 2, \cdots, L_k\}$
Return A_k, G_k

for user k to transmit data on subcarrier m. Then, this data stream is a modified input serial data set of each user, with all the information remapped following the rule created by Algorithm 1. An input x_m from X_k is selected and mapped to the $d_{l,m}$ slot. The final output of the algorithm is interleaving all matrices $\mathbf{D}_k$ to form the final allocation matrix $\mathbf{D}$ which has inputs X remapped in an order of ascending subcarrier index across multiple beams. Fig. 5 illustrates how the re-allocated data reaches the user, as the beam that is pointing directly towards the user is now comprised of subcarriers belonging to 3 different beams.

Algorithm 2 Data Interleaving

Initialise data set $X = \bigcup X_k, k = 1, 2, \cdots, K$ and data allocation matrix $\mathbf{D} = \mathbf{0}^{L \times M}$
Load A_k from Algorithm 1
Insert data into $\mathbf{D}_k = \{d_{l,m} = x_m : x_m \in X_k, l_m = \mathbf{A}_{k,m}, m = 1, 2, \cdots, M\}$
Interleave data $\mathbf{D} = \sum_{k=1}^{K} \mathbf{D}_k$
Return $\mathbf{D}$

V. Results

A. Capacity

Analysis of capacity draws attention towards the increasing number of antennas, as the bandwidth to carrier frequency ratio, ξ, can be static and the number of antennas to improve or optimise performance may vary. Among k UEs, one is selected as a reference UE. In the simulations, user location is randomly generated in the range of $\left[0, \frac{\pi}{2}\right]$ for the reference UE, while the

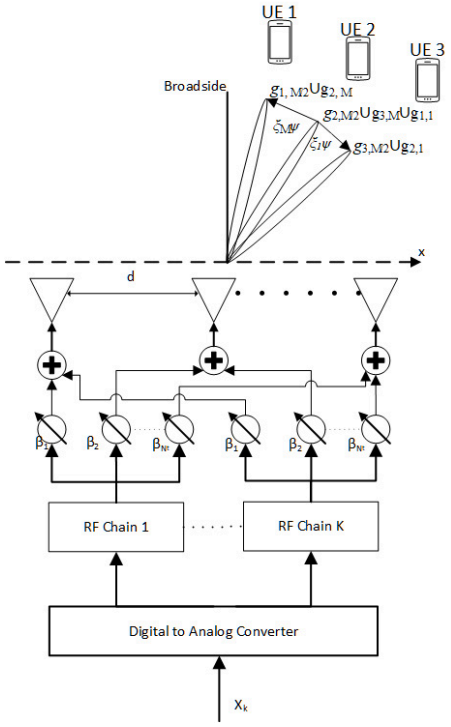

Fig. 5. Stylised solution utilizing different squinted beams for transmission.

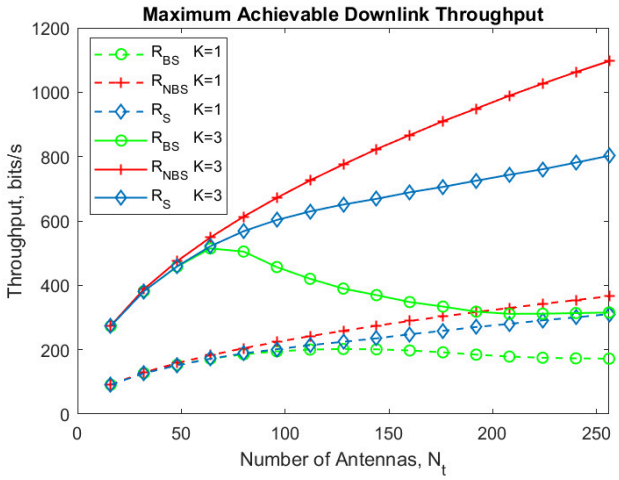

Fig. 6. Maximum achievable DL throughput with solution present for $K = 3$ users scheduled.

other UEs had their positions set to be relative to the reference UE's location. To study the scenario in which performance is significantly affected by beam squint, the correlation between UEs' locations ensures that the three adjacent beams would be signaling towards the three users with maximum gains. Fig. 6 shows, with different number of users in the system, how the number of antennas affects the averaged throughput over different UE locations, as the performance over entire direction range is similar to the proposed algorithm. If Algorithms 1 and 2 are applied, the capacity increases significantly as number of antennas increases, as shown by the result for R_S single user and R_S multi user in Fig. 6. The solution can also be modeled

by modifying (10) to reflect our equivalent gain $G_k[m]$ as

$$R_S = \sum_{k=1}^{K} \frac{B}{M} \sum_{m=1}^{M} \log\left(1 + \frac{P_t \left|G_k\left[m\right]\right|^2}{K\frac{B}{M}N_0}\right). \quad (15)$$

$G_k[m]$ is known to vary as the number of antennas changes and more antennas is equivalent to more beams present in a constant area. As more beams are available, the more resource is available to exploit when squinting occurs. It is important to note the limitation of number of RF chains. Out of K UEs, only $N_{RF}-2$ users will be compensated completely and some data will be re-scheduled for the users that are not fully compensated. Fig. 6 can be examined to see the effects of this, as the sum-rate of the 3 users is not directly 3 times larger than the single user scenario. All of the curves are subject to trends introduced in Section III. To showcase the capacity

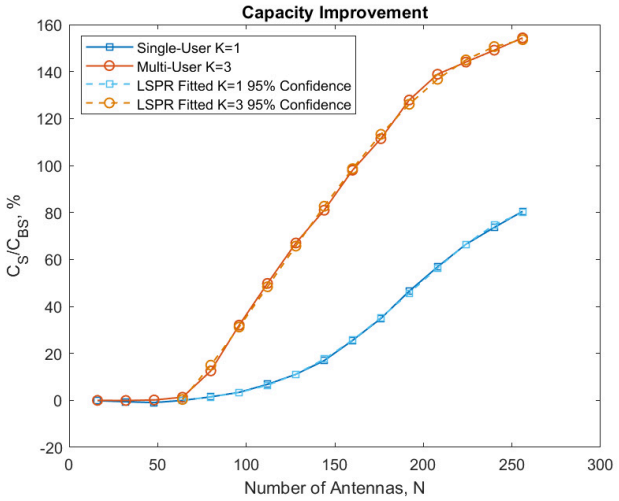

Fig. 7. Capacity improvement for $f_c = 73$GHz, $BW = 2.5$GHz.

effects better an improvement ratio $I = \left(\frac{C_S}{C_{BS}} - 1\right) \cdot 100\%$ is defined, where C_{BS} is acquired from (10). This ratio is shown in Fig. 7. Since the values used for both C_S and C_{BS} are known and present in Fig. 6, Fig. 7 shows that the single user performance for less than 100 antennas is very similar, with slight fluctuation. However, the figures show that if the proposed algorithms are applied to a system with carrier frequency of 73GHz and a wide bandwidth of 2.5GHz, the capacity improves significantly if the number of antennas in a linear array surpasses around 120 antennas for a single user system. A multi-user environment shows a more significant impact as the number of antennas required to see an improvement is reduced to 64. The curve follows a 4^{th} order polynomial function, using Least Squares approximation, with accuracy of 95% :

$$I^K = \begin{cases} 0, & \text{if } N_T < 64 \\ a_4^K N_t^4 + \cdots + a_1^K N_t + a_0^1, & \text{otherwise} \end{cases} \quad (16)$$

where N_t is normalized by $\mu = 160$ and $\sigma = 62.3$. Coefficients are given as $a_4^1 = -2.06, a_3^1 = -3.654, a_2^1 = 10.94, a_1^1 = 34.58, a_0^1 = 25.65$ where K is an index showing the number of users. Due to a more significant increase in performance for multiple user communications, the 3 user case does not strictly improve on I_1 two-fold. As such the coefficients are $a_4^2 = 0.6691, a_3^2 = -4.291, a_2^2 = -10.72, a_1^2 = 59.89, a_0^2 = 98.66$.

VI. Conclusion

In summary, the paper described the analysis of beam squint as a substantial negative effect for an increasing number of antennas and a large bandwidth. It was shown that beam squint significantly affects the capacity of the system. Considering a uniform spacing between beams it was observed that beam squint effect can be exploited. A pair of algorithms were proposed that exploit beam squint for resource allocation. Through simulation it was proved that the solution provides a significant improvement to the system suffering from beam squint, as the number of antennas increases. Furthermore, as the allocation is only conducted within a small number of adjacent beams, the solution is computationally efficient and there is very little change in the complexity of the algorithms as number of antennas or beams increases.

VII. Acknowledgment

This work was supported by the European Union's Horizon 2020 research and innovation programme under grant agreement No 814956 (5G-DRIVE).

References

[1] J. G. Andrews, S. Buzzi, W. Choi, S. V. Hanly, A. Lozano, A. C. K. Soong, and J. C. Zhang, "What will 5g be?" *IEEE Journal on Selected Areas in Communications*, vol. 32, no. 6, pp. 1065–1082, June 2014.

[2] R. W. Heath, N. González-Prelcic, S. Rangan, W. Roh, and A. M. Sayeed, "An overview of signal processing techniques for millimeter wave mimo systems," *IEEE Journal of Selected Topics in Signal Processing*, vol. 10, no. 3, pp. 436–453, April 2016.

[3] H. Zhu and J. Wang, "Chunk-based resource allocation in ofdma systems - part i: chunk allocation," *IEEE Transactions on Communications*, vol. 57, no. 9, pp. 2734–2744, Sep. 2009.

[4] ——, "Chunk-based resource allocation in ofdma systems—part ii: Joint chunk, power and bit allocation," *IEEE Transactions on Communications*, vol. 60, no. 2, pp. 499–509, February 2012.

[5] S. K. Garakoui, E. A. M. Klumperink, B. Nauta, and F. E. van Vliet, "Phased-array antenna beam squinting related to frequency dependency of delay circuits," in *2011 8th European Radar Conference*, Oct 2011, pp. 416–419.

[6] H. Zhu, "Performance comparison between distributed antenna and microcellular systems," *IEEE Journal on Selected Areas in Communications*, vol. 29, no. 6, pp. 1151–1163, June 2011.

[7] M. Cai, J. N. Laneman, and B. Hochwald, "Beamforming codebook compensation for beam squint with channel capacity constraint," in *2017 IEEE International Symposium on Information Theory (ISIT)*, June 2017, pp. 76–80.

[8] G. Li, H. Zhao, and H. Hui, "Beam squint compensation for hybrid precoding in millimetre-wave communication systems," *Electronics Letters*, vol. 54, no. 14, pp. 905–907, 2018.

[9] J. P. González-Coma, W. Utschick, and L. Castedo, "Hybrid lisa for wideband multiuser millimeter-wave communication systems under beam squint," *IEEE Transactions on Wireless Communications*, vol. 18, no. 2, pp. 1277–1288, Feb 2019.

[10] M. Cai, K. Gao, D. Nie, B. Hochwald, J. N. Laneman, H. Huang, and K. Liu, "Effect of wideband beam squint on codebook design in phased-array wireless systems," in *2016 IEEE Global Communications Conference (GLOBECOM)*, Dec 2016, pp. 1–6.